HHS Public Access

Author manuscript

FASEB J. Author manuscript; available in PMC 2025 January 01.

Published in final edited form as:

FASEB J. 2024 January ; 38(1): e23321. doi:10.1096/fj.202301359R.

Perivascular CLICK-gelatin delivery of thrombospondin-2 small interfering RNA decreases development of intimal hyperplasia after arterial injury

Lucas Mota, MD[1], **Max Zhu, BS**[1], **Jennifer Li, MD**[1], **Mauricio Contreras, MD**[1], **Tarek Aridi, MD**[1], **John N. Tomeo, B.S**[1], **Alexander Stafford, Ph.D**[2], **David J. Mooney, PhD**[2], **Leena Pradhan-Nabzdyk, PhD**[1], **Christiane Ferran, MD, PhD**[1,3,4], **Frank W. LoGerfo, MD**[1], **Patric Liang, MD**[1]

[1.]Division of Vascular and Endovascular Surgery, Beth Israel Deaconess Medical Center, Boston MA

[2.]John A. Paulson School of Engineering and Applied Science, Harvard University, Cambridge, MA

[3.]The Center for Vascular Biology Research, Beth Israel Deaconess Medical Center, Boston MA

[4.]Division of Nephrology, Department of Medicine, Beth Israel Deaconess Medical Center, Boston MA

Abstract

Bypass graft failure occurs in 20-50% of coronary and lower extremity bypasses within the first-year due to intimal hyperplasia (IH). TSP-2 is a key regulatory protein that has been implicated in the development of IH following vessel injury. In this study, we developed a biodegradable CLICK-chemistry gelatin-based hydrogel to achieve sustained perivascular delivery of TSP-2 siRNA to rat carotid arteries following endothelial denudation injury. At 21 days, perivascular application of TSP-2 siRNA embedded hydrogels significantly downregulated TSP-2 gene expression, as well as other associated mediators of IH including MMP-9 and VEGF, ultimately resulting in a significant decrease in IH. Our data illustrates the ability of perivascular CLICK-gelatin delivery of TSP-2 siRNA to mitigate IH following arterial injury.

Graphical Abstract

Corresponding Author: Patric Liang, MD, Beth Israel Deaconess Medical Center, 110 Francis St. Suite 5B, Boston, MA 02215, Phone: 617-632-9848, pliang1@bidmc.harvard.edu.

Author Contributions:

LM, MZ, JL, LPN, CF, FWL and PL contributed to the conception of the study. LM, MZ, LPN, CF, FWL and PL contributed to the design of the experiments. LM, MZ, JL, TA and JNT performed the research and acquired the data. LM, LPN, FWL and PL contributed to the supervision of the studies and data review. LM, TA, and MZ analyzed and interpreted the data. All authors reviewed and edited the manuscript and provided approval on the final submitted version.

Conflict of Interest Statement:

The authors declare no conflict of interest.

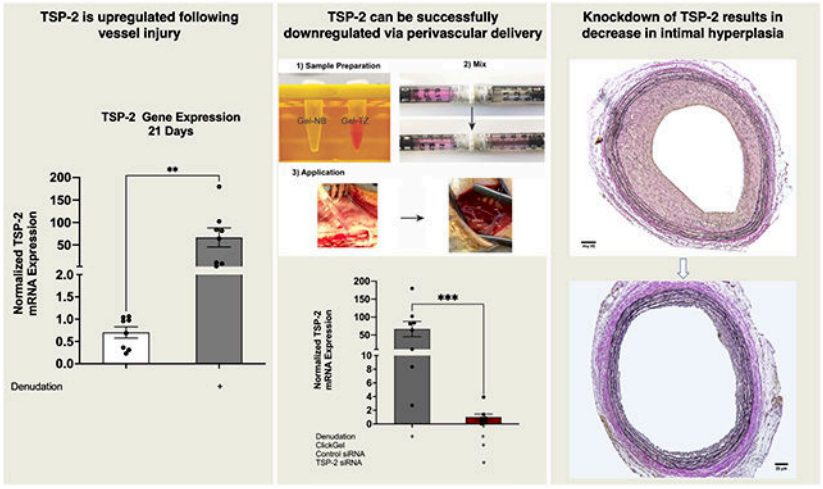

At 21 days following vessel denudation TSP-2 is upregulated and significant intimal hyperplasia is observed. Following application of TSP-2 siRNA embedded CLICK-gelatin, TSP-2 is downregulated and a significant decrease in intimal hyperplasia is observed.

Introduction

Atherosclerotic cardiovascular disease affects more than 18.3 million people in the United States, has an estimated global adult prevalence rate of 9.8%, and commonly manifests as peripheral arterial disease (PAD) or coronary artery disease (CAD) (1-3). PAD can lead to limb threatening ischemia as disease severity worsens, resulting in lower extremity rest pain, non-healing ulcers, gangrene, and ultimately limb loss unless a revascularization procedure is successfully performed (4, 5). Similarly, revascularization is indicated when CAD results in unstable angina or myocardial infarction (6, 7). Autologous vein is the gold standard conduit for surgical lower extremity bypass surgery and the leading conduit used for coronary artery bypass surgery (8, 9). However, 20-40% of lower extremity vein grafts and 20-50% of coronary bypasses suffer from conduit failure within the first year (10-13). The pathophysiology of bypass graft failure has been linked to the development of intimal hyperplasia (IH), which can occur throughout vein grafts, but predominates at the distal graft anastomosis of prosthetic bypass grafts (14-16). Anastomotic IH is likely triggered by iatrogenic injury to the vessel wall at the time of surgery and changes in biomechanical stress following bypass, which damages the integrity and function of the arterial endothelial cell (EC) and medial smooth muscle cell (SMC) layers. On a molecular level, this results in maladaptive changes in vascular gene expression that culminate in a phenotypic transformation of endothelial cells from quiescent to inflammatory and prothrombotic, and of smooth muscle cells from contractile to migratory and secretory (15, 17, 18). Ultimately, smooth muscle cell migration from the media to the intima coupled with excessive cell proliferation of extracellular matrix leads to the development of IH. Histologically, several markers have been identified to identify the pathologic development of IH such as Ki-67, a marker for cell proliferation, CD31 and VEGF-R2, markers for adventitial neovascularization, and MMP9, a maker for vascular injury and inflammation (19-22). However, despite the understanding of IH as a key culprit of graft failure, minimal

scientific and translational progress has been made to successfully target the key regulators of graft failure and improve bypass graft patency (23, 24).

We previously identified a heightened and sustained upregulation of thrombospondin-2 (TSP-2) at the distal bypass graft anastomosis in canine models following bypass surgery (25). TSP-2 is an extracellular matrix protein that is a key modulator in the pro-atherogenic switch of both EC and SMC phenotypes and is a key regulator in the development of IH (25-27). We have therefore sought to downregulate TSP-2 expression in both EC and SMC layers of the vessel wall. In previous *in vitro* studies, we demonstrated successful transfection of TSP-2 siRNA in human aortic smooth muscle cells with protein knockdown up to 30 days (27). Using *in vivo* rat models, we demonstrated upregulation of TSP-2 gene and protein expression following injury-induced arterial IH, that was reduced by intraluminal delivery of TSP-2 siRNA along with a decrease in the severity of IH lesions at 21 days (28). However, this method of intraluminal delivery of TSP-2 siRNA directly into the vein graft is short-lived, requires prolonged vein distension, which may lead to additional endothelial injury, and cannot be used to treat prosthetic grafts given its acellular nature. We, therefore, developed a novel biologic vascular gene delivery system, utilizing a biodegradable gelatin-based hydrogel. This hydrogel is applied extraluminally at the time of surgery, to direct sustained perivascular delivery of gene therapy to all layers of the arterial wall, such as TSP-2 siRNA.

The purpose of this study is to evaluate the efficacy of *in vivo* perivascular delivery of TSP-2 siRNA to the arterial wall using a tetrazine (Tz)-norbornene (NBr) CLICK-chemistry based hydrogel delivery platform in a rat carotid artery balloon angioplasty model. Specific objectives include confirming effective delivery of siRNA with knockdown of TSP-2 gene transcription and protein translation, as well as the ability to reduce the IH response following arterial injury. This study was designed and performed in anticipation of future translation for treatment of bypass grafts in large animal studies.

Materials and Methods:

siRNA design and transfection agent:

Rat-specific TSP-2 siRNA, nontargeting control siRNA, and human-specific GAPDH siRNA were obtained from Thermo Fisher Scientific (Waltham, MA, USA). Polyethylenimine (PEI; *in vivo* jetPEI/*in vitro* jetPRIME; Polyplus, Strasbourg, France) was used as the transfection reagent. Horizon Discovery (Lafayette, LA, USA) supplied the siGLO red transfection indicator. Information about siRNA and siGLO is provided in supplemental Table 1.

CLICK-Hydrogel

For CLICK-gelatin polymer preparation, high bloom, low endotoxin Type A gelatin was modified with 3-(p -benzylamino)-1,2,4,5-tetrazine (Tz) and 5-norbornene-2-methylamine (Nb) in the presence of 1-ethyl-3-(3-dimethylaminopropyl)-carbodiimide hydrochloride (EDC) to produce Gelatin-Tz and Gelatin-Nb, respectively (Figure 1A,B). Gelatin polymer solutions conjugated with norbornene or tetrazine functional groups were combined in a 1:1

ratio in 1X phosphate buffered saline (PBS) to achieve a 5% (w/v) hydrogel. Cross-linking occurs via a tetrazine-norbornene CLICK-chemistry reaction when mixed, achieving rapid gelation within 10 seconds and avoids reactivity with loaded siRNA. PEI and siRNA were dissolved into CLICK-gelatin solutions prior to polymerization.

For CLICK-alginate polymer preparation, medium viscosity alginate (MVG, NovaMatrix) was modified with 3-(p -benzylamino)-1,2,4,5-tetrazine (Tz) and 5-norbornene-2-methylamine (Nb) in the presence of 1-ethyl-3-(3-dimethylaminopropyl)-carbodiimide hydrochloride (EDC) to produce Alginate-Tz and Alginate-Nb, respectively.

Cell culture and reagents

Human Aortic Endothelial Cells (HAoECs, Lonza, Walkersville, MD) passages 3 to 6 were cultured in growth media consisting of Vasculife HAoEC basal medium supplement with Vasculife Life Factors kit (Lifeline Cell Technology, Walkersville, MD), 5% fetal bovine serum (Hyclone, Logan, UT), and Dulbecco's Modified Eagle's Medium (DMEM) consistent of low glucose, L-glutamine, and sodium pyruvate (Invitrogen, Carlsbad, CA). Assays were performed in 24-well plates (Corning, Lowell, MA) with initial seeding density of 25,000 cell per well.

siRNA Mediated *in vitro* Gene Knockdown

HAoECs were transfected 24 hours after plating using the transfection reagent, JetPEI (Polyplus, Strasbourg, France) and siRNAs targeting GAPDH (Thermo Fisher Scientific, Waltham, MA, USA). *In vitro* transfection was performed per the manufacturer's protocol. The negative control group was untreated HAoECs (NT) and positive control group was HAoECs transfected with JetPEI + siGADPH in normal growth media (50nM). Treatment groups were HAoECs transfected with JETPEI + siGADPH in the presence of 500μL growth media containing 0.6mg of either alginate, CLICK-alginate-Tz, CLICK-alginate-NBr, gelatin, CLICK-gelatin (Tz), or CLICK-gelatin (NBr) polymers. Transfection was allowed for 48 hours prior to cell harvest.

Animal Model and Surgical Procedure:

Protocols for this study were approved by the Institutional Animal Care and Use Committee at Beth Israel Deaconess Medical Center, and all animals were treated in compliance with the *Guide for the Care and use of Laboratory Animals* (NIH, Bethesda, MD, USA). Both male and female adult retired breeder Wistar rats (Charles River, Indianapolis, IN, USA) were used at an ideal weight of 450-500 and 325-350 g, respectively (n = 8 rats per group). Sample size was determined based on previous experience. One CCA was injured utilizing a balloon denudation model (14). Details about the balloon injury model are provided in the Supplementary Section. Following injury, the balloon-injured region of the CCA, measuring 1cm approximately, was circumferentially coated with CLICK-gelatin infused with either nontargeting control siRNA with PEI (Control siRNA), anti-TSP-2 siRNA (TSP-2 siRNA) with PEI (both 7.5μM), or CLICK-gelatin alone. To assess siRNA delivery *in vivo* CLICK-gelatin embedded with siGLO +PEI (7.5μM) was used. For denuded non-treated (NT) group, the common carotid was externally irrigated with saline following injury, and this served as overall positive control. After treatment, hemostasis was achieved, and the wound

was approximated in two layers with a running suture (5-0 Vicryl Plus). Extended-release Meloxicam was administered as postoperative analgesia (2mg/kg i.p). Rats transfected with siGLO were analyzed to determine depth of siRNA transfection in this model.

Tissue Harvest:

At 21 days after the surgical procedure, rats were placed under deep anesthesia. Dissection was carried out and the denuded CCA along with contralateral non-denuded CCA were then harvested and placed in 10% formalin at 4°C for 24 hours for further fixation. Before embedding in paraffin, the vessels were transferred to saline, and each CCA was cut at its midpoint, such that the analysis started at the midsegment of the denudation. Rats transfected with siGLO were harvested after 2d to prevent degradation of the Cy3 fluorescence signal and these tissue samples were frozen in O.C.T. compound (Thermo Fisher Scientific) for frozen IF.

Quantitative real-time PCR

RNA was isolated from HAoEC culture using the RNEasy Mini kit (Qiagen Inc., Valencia, CA) for *in vitro* experiments. Similarly, for *in vivo* experiments, RNA was isolated from paraffin embedded tissues using the Recoverall Total Nucleic Acid Isolation Kit for FFPE (Thermo Fisher Scientific) and purified using an RNA Clean & Concentrator kit (Zymo Research, Irvine, CA, USA). RNA was quantified using a NanoDrop spectrophotometer. 100ng of RNA from each sample was used for cDNA synthesis using an iScript cDNA synthesis kit (Bio-Rad, Hercules, CA, USA). Gene expression was quantified using quantitative real-time PCR (qRT-PCR). Human-specific primers for GAPDH and the housekeeping gene beta-actin (BA) as well as rat-specific primers for TSP-2 and the housekeeping gene, β_2 macroglobulin (B2M), were obtained from Integrated DNA Technologies (Coralville, IA, USA). GAPDH and TSP-2 mRNA levels were normalized to BA and B2M expression, respectively, for each sample using the $2^{-\mathrm{DD}Ct}$ method. For the in vivo studies, experimental groups were compared to non-denuded contralateral CCA. Information about the reagents and primer sequences is provided in supplemental Table 1.

Histology

Paraffin-embedded tissues were sectioned into 6 μm cross-sections for histological staining. Verhoeff Von Giesson staining (Newcomer Supply, Middleton, WI, USA) was performed to identify the elastic lamina. ImageJ (Bethesda, MD, USA) was used to calculate the area of the intima and media layers of each CCA, which were subsequently used to calculate intima-to-media (I/M) ratios as a marker of IH. Analysis included the same n=8 rats per group used for qRT-PCR analysis. Collagen deposition was assessed with Masson's Trichrome stain and presented as a percentage of the total area. Prior to analysis, images were deidentified in order to allow for blinded assessment. Information about the reagents is provided in Supplemental Table 1.

Immunohistochemical analysis

Immunofluorescence (IF) staining was performed to assess siGLO delivery, as well as for TSP-2, matrix metalloproteinase 9 (MMP9), platelet endothelial cell adhesion molecule

(PECAM-1/CD31), and antigen Kiel 67 (Ki-67) protein expression. Immunohistochemistry (IHC) staining was performed for vascular endothelial growth factor receptor (VEGF-R2) and cluster of differentiation 68 (CD68) protein expression. Information about specific antibodies, reagents is provided in Supplemental Table 1. The expression levels for IHC and IF were determined by calculation with ImageJ software (Bethesda, MD, USA) for dissemination (percentage area of vessel with positive signal) and integrated density (sum of all pixel values with positive signal in an area). Contralateral CCA which were not denuded were used as the negative control group for these experiments. Prior to density and dissemination calculation images were deidentified in order to allow for blinded assessment of IHC signal. Positive staining of MMP9 was observed predominantly in the adventitia, and therefore only staining density was quantified.

TUNEL staining

In situ terminal deoxynucleotidyl transferase mediated dUTP nick-end labelling (TUNEL) was performed using an in-situ apoptosis kit (VasoTACS, Bio-Techne) to localize cells undergoing nuclear DNA fragmentation in paraffin-embedded sections according to manufacturer's instruction. The presence of apoptotic cells was identified as dark nuclear staining. The images were captured at 100×, 200× and 400× magnification and number of positive apoptotic cells and bodies were determined utilizing ImageJ cell counter. Right CCA which were not denuded were used as the negative control group for these experiments. Images were deidentified and randomized prior to counting.

Statistical Analysis

All statistics were performed using GraphPad Prism (San Diego, CA, USA). T-tests were used to compare non-denuded contralateral CCA to denudation only CCA. One-way ANOVA with post-hoc Tukey tests were used for analysis comparing different denudation groups. Sample size determination was based on previous experiments and post hoc power analysis was conducted to ensure the chosen sample size was sufficient to provide a statistical significance of $P<0.05$ with a 90% probability. All tests were 2-sided, and data was considered statistically significant at $P<0.05$.

Results:

Study Design Rationale.

This study was performed to evaluate whether perivascular delivery of TSP-2 siRNA could prevent the development of IH in a rat common carotid artery (CCA). This objective was addressed by (i) testing the efficacy of GAPDH siRNA delivery to human aortic endothelial cells (HAoECs) using biocompatible hydrogels, namely alginate and gelatin, to determine the optimal delivery hydrogel polymer, ii) confirming *in vivo* perivascular delivery to rat CCA utilizing CLICK-gelatin embedded with siGLO (control siRNA with a Cy3 fluorescence tag), iii) inducing IH via balloon denudation injury of CCA, analyzing changes in TSP-2 gene and protein expression, and the impact of perivascular CLICK-gelatin delivery of TSP-2 siRNA on the observed changes, iv) examining the impact of CLICK-gelatin delivery of TSP-2 siRNA on vascular injury/inflammatory pathways, and v) determining the extent of IH at 21 days following denudation in each experimental group.

Gelatin versus alginate hydrogels for siRNA delivery

CLICK-chemistry was utilized to design hydrogels that would allow for rapid gelation without the need for external energy input, and thus reduce the risk of disrupting siRNA from polyethylenimine (PEI), an siRNA transfection agent (Figure 1A,B). Gelatin and alginate are two polymers that are widely used in medicine and have comparable biocompatibility profiles. To determine an optimal hydrogel polymer for siRNA delivery, we tested GAPDH mRNA expression following transfection with GAPDH siRNA in the presence of media containing gelatin or alginate polymers as well as their individual CLICK-modified components. GAPDH, a housekeeping gene, was utilized instead of TSP2 due to its universal expression without need for cell stress or injury.

48 hours after GAPDH siRNA + PEI transfection, HAoECs that were transfected in media containing raw gelatin (0.24 ± 0.02), CLICK-Gelatin Tz (0.12 ± 0.02, $p<0.001$), and CLICK-Gelatin NBr (0.11 ±0.01, $p<0.001$) demonstrated significant reduction in GAPDH mRNA expression, compared to non-treated AoECs (NT) (Figure 1C). Transfection efficiency was no different for AoECs transfected in media containing gelatin ($p=0.440$), CLICK-gelatin Tz ($p=0.994$) or CLICK-gelatin NBr ($p=0.999$) compared with AoECs transfected with siGAPDH+PEI in normal growth media (0.06 ± 0.01). In contrast, there was no significant reduction in GAPDH mRNA expression following transfection in the presence of media containing alginate (1.03 ±0.07, $p=0.999$) or CLICK-Alginate Tz (1.13 ± 0.06, $p=904$), except CLICK-Alginate NBr containing media (0.42 ± 0.07, $p<0.001$). Given the lack of interference of siRNA transfection in the presence of CLICK-gelatin polymers, CLICK-gelatin was selected as the optimal delivery platform for *in vivo* perivascular siRNA delivery.

siRNA transfection dissemination via CLICK-gelatin delivery

CLICK-gelatin siRNA transfection efficacy *in vivo* was assessed by quantifying the depth of siGLO epifluorescence.

48 hours after siGLO delivery via CLICK-gelatin to the denuded artery (Figure 2A), fluorescence microscopy demonstrated significant penetration of siGLO in the adventitia, with some penetration into the media (Figure 2B,C).

Effect of arterial denudation on TSP-2 gene and protein expression, and IH

TSP-2 gene expression was measured by quantitative real-time PCR (qRTPCR) at 21 days after the injury procedure and treatments. To confirm model validity, TSP-2 gene and protein expression, and development of IH was first compared between non-denuded CCA and denuded NT CCA at 21 days (N=8 per group).

21 days after denudation, TSP-2 gene expression was significantly up-regulated in denuded NT group (66.71, ± 60.08) compared with non-denuded CCA (1.00 ± 0.3; $p<0.001$), which was also reflected with increase in TSP-2 protein expression (Figure 3A,B). At 21 days, the intima/media area ratio was significantly increased in denuded NT CCA (1.36, ± 0.14) compared with non-denuded CCA (0.074, ± 0.003; $p<0.001$) (Figure 3C,D), confirming the validity of this IH model.

Effect of TSP-2 siRNA transfection on TSP-2 gene expression

To investigate the impact of TSP-2 siRNA perivascular delivery utilizing CLICK-gelatin on TSP-2 gene expression *in vivo*, CCA were analyzed at 21 days after denudation and treatment with CLICK-gelatin, CLICK-gelatin + control siRNA, or CLICK-gelatin + TSP-2 siRNA. PCR data are normalized to non-denuded CCA and expressed as fold change. Non-denuded CCA was the negative control (n=8) and denuded untreated CCA (denuded NT, n=8) was the positive control. Experimental groups were as follows: denuded CCA with CLICK-gelatin alone (n=8), denuded CCA with CLICK-gelatin + control siRNA (n=8), and denuded CCA with CLICK-gelatin + TSP-2 siRNA (n=8).

At 21 days, there was a significant reduction in TSP-2 mRNA expression in the CLICK-gelatin + control siRNA (4.11, ± 1.78, p=0.002), and CLICK-gelatin + TSP-2 siRNA (1.01 ± 1.26; p<0.001) groups compared with the denuded NT (66.7 ± 21.2) CCA group (Figure 4A). CLICK-gelatin + TSP-2 siRNA group had a significant decrease in in TSP-2 expression compared with CLICK-gelatin + control siRNA (p=0.004) group (Figure 4B).

Effect of TSP-2 siRNA transfection on TSP-2 protein expression.

At 21 days, TSP-2 protein expression was compared between denuded NT, CLICK-gelatin alone, CLICK-gelatin + control siRNA, and CLICK-gelatin + TSP-2 siRNA groups by Immunofluorescence (IF) (n=4 per group). Quantification of TSP-2 protein expression was based on density and dissemination of the fluorescence signal in the CCA.

Compared with the denuded NT CCA (87.2 ± 10.7) at 21 days, TSP-2 protein density was significantly reduced in vessels treated with CLICK-gelatin + control siRNA (55.4 ± 9.46, p=0.026), and CLICK-gelatin + TSP-2 siRNA treatment (23.9 ± 4.91, p<0.001) (Figure 5A,B). Additionally, TSP-2 protein density was significantly reduced in the CLICK-gelatin + TSP-2 siRNA treatment, compared with CLICK-gelatin + control siRNA groups (p=0.027) (Figure 5A,B). In terms of dissemination area, CLICK-gelatin + TSP-2 siRNA (0.362 ± 0.0454, p<0.001) groups were associated with a significant decrease in TSP-2 protein expression, compared to denuded NT (1.46 ± 0.244). CLICK-gelatin + TSP-2 siRNA was also associated with a decrease in TSP-2 protein dissemination, compared with CLICK-gelatin + control siRNA (1.13 ±0.148, p=0.007) (Figure 5A,C).

Effect of TSP-2 siRNA transfection on regulation of MMP-9

MMP9 protein expression was investigated because it is an extracellular matrix remodeling protein that is impacted downstream by TSP-2 expression and is known to play a role in vascular injury.

We analyzed MMP-9 protein expression at 21 days by IF (n=4 per group).

At 21 days, compared with the denuded NT (139 ± 13.0) group, the CLICK-gelatin + control siRNA (87.9 ± 10.9, p=0.021) and CLICK-gelatin + TSP-2 siRNA(44.7 ± 6.73, p<0.001) treatment groups resulted in a significant reduction in MMP-9 protein density (Figure 6A,B). Additionally, MMP-9 expression was significantly lower in CLICK-gelatin + TSP-2 siRNA group, compared to CLICK-gelatin + control siRNA (p=0.043) groups (Figure 6A,B).

Effect of TSP-2 siRNA transfection on regulation of CD31 and VEGF-R2

CD31 (IF) and VEGF-R2 (immunohistochemistry) expression at 21 days (n=4 per group) following denudation was investigated to determine the role of TSP-2 siRNA in regulating adventitial neovascularization.

At 21 days, CLICK-gelatin + control siRNA (65.5 ± 7.98, p=0.005), and CLICK-gelatin + TSP-2 siRNA treatment (26.7 ± 1.82, p<0.001) significantly reduced neovascularization, represented by density of CD31, in adventitia compared to the denuded NT group (107 ± 12.8) (Figure 7A,B). This reduction was particularly evident in vessels treated with CLICK-gelatin + TSP-2, which also demonstrated a significant reduction in CD31 expression compared to CLICK-gelatin + control siRNA (p=0.009) group (Figure 7A). Correlating with reduced adventitial neovascularization, there were significantly fewer VEGF-R2 expressing cells in CLICK-gelatin + TSP-2 siRNA group (16.3 ± 4.85, p<0.001), and CLICK-gelatin + control siRNA groups (46.4 ± 3.20, p<0.001), compared with the denuded NT (104 ± 11.7) group (Figure 8A,B). VEGF-R2 expressing cells were significantly lower in the CLICK-gelatin + TSP-2 siRNA group, compared with the CLICK-gelatin + control siRNA (p=0.01) groups.

Effect of TSP-2 siRNA transfection on macrophage infiltration

To identify inflammatory events, we examined CCA for infiltration of macrophages at 21 days after transfection by immunostaining for CD68 antigen. Data are expressed as $CD68^{+}$ integrated density.

21 days after denudation there was a significant decrease in macrophage infiltration in CLICK-gelatin + TSP-2 siRNA (9.5 ± 1.0, p<0.001) and CLICK-gelatin + control siRNA (26.4 ± 6.4, p=0.005) groups compared to denuded NT group (48.2 ± 3.3; Figure 9A). CCA treated with CLICK-gelatin + TSP-2 siRNA also demonstrated a significant reduction in macrophage infiltration compared to CLICK-gelatin + control siRNA (p=0.020). Representative images of macrophage infiltration are depicted in Figure 9B.

Effect of TSP-2 siRNA transfection on cellular proliferation

Cell proliferation is a key event in the development of IH. Immunostaining for Ki-67, a marker of cellular proliferation, was performed in all CCA at 21 days. Data are presented as integrated density of fluorescent signal and percentage of proliferating cells per total CCA area.

21 days after denudation cell proliferation, represented by Ki-67 signal density, was significantly reduced in CLICK-gelatin + TSP-2 siRNA treated groups (5.4 ± 2.2) compared to denuded NT group (54.7 ± 18.6, p=0.011; Figure 10A). Percentage of proliferating cells was also significantly reduced in CLICK-gelatin + TSP-2 siRNA treated groups (0.1 ± 0.03%) compared to denuded NT group (1.4 ± 0.5%, p=0.018; Figure 10B). There was no significant difference between CLICK-gelatin + TSP-2 siRNA and CLICK-gelatin + control siRNA in either density (23.0 ± 12.1, p=0.306) or percentage area (0.6 ± 0.1%, p=0.614) of proliferating cells. Representative images of cellular proliferation are depicted in Figure 10.

Effect of TSP-2 siRNA transfection on cell apoptosis

SMC and EC apoptosis has been linked with induction of vascular remodeling and SMC migration, thus contributing to IH formation (29, 30). Apoptotic cells were determined via TUNEL staining a 21 d. Data are presented as total number of apoptotic cells/bodies.

21 days after denudation, there was a significant decrease in the number of apoptotic cells in CCA treated with CLICK-gelatin + TSP-2 siRNA (11.3 ± 2.2) compared to denuded NT (109.3 ± 22.1, p=0.001) and CLICK-gelatin + control siRNA (62.3 ±12.7, p=0.037) groups. Representative images of cellular proliferation are depicted in Figure 11B.

Effect of TSP-2 siRNA transfection on collagen deposition

Given that a significant proportion of the final IH lesion is made up of collagen, collagen deposition was measured using Masson's Trichrome stain at 21 days (n=4 per group). Data are presented as area of collagen stained in intima as percentage of entire area of vessel.

21 days after denudation, CLICK-gelatin + TSP-2 siRNA treated groups (26.8 ± 3.9%) demonstrated significant reduction in collagen deposition compared to denuded NT group (53.5 ± 7.5%, p=0.002) (Figure 12A,B). Although there was no statistical reduction in collagen deposition in CLICK-gelatin + TSP-2 siRNA treatment compared to CLICK-gelatin + control siRNA (39.9 ± 1.7%, p=0.08) groups, there was a trend towards decreased collagen deposition expression in the CLICK-gelatin + TSP-2 siRNA group (Figure 12A).

Effect TSP-2 siRNA transfection on IH

The effects of TSP-2 silencing on IH were evaluated by measuring intima/media area ratios of specimens stained using Verhoef-Van Giesson stain at 21 days (n=8 per group).

The CLICK-gelatin + TSP-2 siRNA treatment group (0.591 ± 0.108) demonstrated a significant reduction in the intima/media area ratio compared to the denuded untreated (1.42, ± 0.0594; p<0.001), and CLICK-gelatin + control siRNA treated groups (1.19, ± 0.108; p=0.003) (Figure 13A,B). There was no statistical difference in intima/media ratio between the denuded untreated group, and the CLICK-gelatin + control siRNA treated groups (p=0.243) (Figure 13A).

Discussion:

In this study we demonstrated that siRNA can be successfully delivered to suppress a target gene using a perivascular CLICK-gelatin hydrogel delivery system. Specifically, we found that perivascular delivery of TSP-2 siRNA results in a decrease in IH and associated collagen deposition at 21 days following arterial injury in a rat carotid angioplasty model. Furthermore, we demonstrated reduction of TSP-2 gene and protein expression at 21 days following TSP-2 siRNA transfection. TSP-2 siRNA transfection also led to a significant decrease in MMP-9 protein expression, neovascularization, inflammation, proliferation, and cell death.

These findings expand on our prior work demonstrating the ability of intraluminal arterial delivery of TSP-2 siRNA to effectively modulate MMP-9, a protein known to play a role in

IH (31, 32). Our current work similarly demonstrates effective silencing of TSP-2 at 21 days from a perivascular approach, resulting in a decrease in its downstream targets including MMP-9. Whereas we did not find a statistically significant reduction in I:M ratio using our prior transient intraluminal delivery methods, this novel perivascular delivery using a CLICK-gelatin delivery system resulted in a more significant reduction in IH after arterial injury. These findings support the need for sustained TSP2 suppression following initial injury, which can be achieved using a biodegradable gelatin-based hydrogel. Furthermore, this perivascular approach avoids the need for intraluminal siRNA transfection with vessel distention, which can lead to inadvertent toxicity and loss of ECs and SMCs (33-35). An external biologic delivery system is also more compatible with use in prosthetic materials given its ability to be applied perivascularly around a vessel anastomosis.

TSP-2, which is primarily produced by SMC and fibroblasts, has been described to be an important modulator of cell-matrix interactions and regulator of SMC and EC proliferation (27, 36). TSP-2 role in increasing SMC proliferation, a key step in the formation of IH, has been clearly described (37, 38). Our study suggested that downregulation of TSP-2 inhibits this dysregulated proliferation of cells, as demonstrated by the decrease of Ki-67 in CCA treated with CLICK-gelatin + TSP-2 siRNA. Further supporting inhibition of cell proliferation as an important mechanism of TSP-2 downregulation in attenuating IH formation. TSP-2 has been shown to regulate the pro-atherogenic switch of EC and SMC phenotypes, thus playing a crucial role in the development of IH (26). This effect of TSP-2 is likely achieved through its modulation of extracellular matrix proteins such as MMP-9. MMP-9 has been demonstrated to be upregulated by TSP-2, enhancing cell migratory potential, leading to SMC migration and replication (39-41). Therefore, we hypothesize that regulation of MMP-9 expression following injury is likely modulating the cellular response leading to IH. Our data supports this model of IH development since TSP-2 silencing led to a statistically significant decrease in MMP-9 expression and decrease in IH at 21 days.

In addition to modulating cell migratory potential through its effect on MMP-9 expression, TSP-2 siRNA may also play a protective role against IH by decreased adventitial neovascularization. Adventitial revascularization has been associated with increase in neointima thickness in stenotic vein grafts and angioplasty models (42-44). Furthermore, pathological neovascularization, has also demonstrated to play a role in the recruitment of inflammatory cells, leading to high intimal macrophage content, contributing to IH (45, 46). The decrease in adventitial neovascularization demonstrated by TSP-2 knockdown in this study is likely modulated via MMP-9. MMP-9 has been implicated in recruitment of endothelial cells and proliferation associated with angiogenesis through its role in the transforming growth factor beta pathway and in mobilizing VEGF from the ECM (47, 48). In fact, MMP-9 has been shown to possess a positive correlation with the degree of neovascularization in carotid plaques (48). Given the association of neovascularization with presence and progression of IH and atherosclerosis, it is possible that prevention of neovascularization, via decrease in MMP-9, is another pathway through which TSP-2 siRNA reduces IH (49-51).

Furthermore, TSP-2 siRNA also affects monocyte and macrophage infiltration. In the CLICK-gelatin + TSP-2 siRNA group, we observed a decrease in CD68 expressing cells

compared to our control groups. Macrophages contribute to the formation of IH via multiple mechanism, from local inflammation and foam cell transformation to production of proinflammatory cytokines, such as IL-1, IL-18 and TNF-a, and matrix metalloproteinases, which degrade the basement membrane (52-54). TSP-2 acts as a competitive antagonist of TSP-1 mediated TGF-ß1 activation (55). Therefore, by silencing TSP-2, there is an increase in activated TGF-ß1, which results in the decrease in proinflammatory macrophage phenotype, and suppression of macrophage migration, as suggested in our study (28, 56). However, given previous studies demonstrated the paradoxical stimulatory and inhibitory nature of TGF-ß on macrophages, further studies are needed to better understand the mechanisms of TSP-2 in macrophage regulation (57, 58).

TSP-2 siRNA also appears to prevent apoptosis in CCA following denudation. Thrombospondin family proteins, particularly TSP-1, have been shown to induce apoptosis (59, 60). TSP-2's specific role in controlling apoptotic pathways remains controversial, with some studies suggesting TSP-2 may not play a role at all in apoptotic pathways or in inhibiting apoptosis (61, 62). Our results however appear to support TSP-2 role in inducing apoptosis as previously demonstrated *in vitro* by Koch et al and Bartoli et al where TSP-2 induced apoptosis via activation of caspase 3 (63, 64). This reduction in apoptosis may play an important role in TSP-2 silencing leading to reduction of intimal hyperplasia. This could possibly happen due to the decrease in cell death preventing a cellular overresponse that leads to the formation of the neointimal lesion (65, 66). Additionally, the reduction in vascular SMCs apoptosis also prevents the rapid decrease in vessel wall cellularity that typically follows acute injury, and thus preventing the migration of SMCs to the intima, an important step in intimal hyperplasia formation (65).

The present study also demonstrates effective TSP-2 siRNA transfection, with silencing of the TSP-2 gene at 21 days after siRNA delivery using CLICK-gelatin. Although perivascular delivery presents a clear advantage in terms of localized and sustained delivery and reduced graft injury, it may pose a logistic issue intraoperatively. Commercial gelatin hydrogels are not compatible with our gene therapy platforms due to cross-reactivity with the biologics during the crosslinking gelation process, while other forms of gel-based delivery mechanism often require external energy input, which may not be feasible and likely unsafe in an intraoperative setting. Our use of CLICK-gelatin eliminates the need for external energy input and relies on copper-free, inverse electron-demand Diels-Alder (IEDDA) CLICK reactions between Tz and NBr (67). Furthermore, CLICK-gelatin exhibits rapid gelation and high degree of chemo-selectivity, ensuring surgical application while preserving integrity of biologics. Additionally, as demonstrated in this study, gelatin is a superior siRNA delivery polymer compared with other commonly used polysaccharides such as alginate. This is likely explained by competing strong negative charges from the alginate compound, which competes with negatively-charged siRNA to complex with positively-charged PEI (68). Therefore, for delivery of siRNA complexes, neutrally charged polysaccharides such as gelatin should be preferred. This novel method of perivascular siRNA does not require any modifications of surgical techniques or graft materials and would likely not increase operating room time significantly, making it a promising delivery mechanism for vascular gene therapy.

Contrary to expectation, we did not visualize siRNA transfection into the tunica intima in this study. Most of the signal visualized using siGLO transfection was limited to the adventitia with some penetration into the media. Given the decreasing visualization quality of siGLO after 24 hours, and the maximum siRNA transfection occurring at 48 hours post-delivery, it is possible that transfected cells in the intima were not adequately visualized (69, 70). However, it is more likely that due to the increased length of penetration that is required utilizing a perivascular delivery system, as opposed to intraluminal delivery, and the short half-life of the siGLO red fluorophore, signal may have degraded prior to reaching the inner most layer of the vessel. However, the significant reduction in IH seen at 21 days using perivascular delivery of TSP-2 siRNA, which was not previously seen with intraluminal delivery, suggests that perivascular delivery can lead to clinically favorable outcome of reduction in IH. Since TSP-2 is primarily produced by SMCs and fibroblasts, targeting the adventitia and media layers where these cells are found may be of greater importance.

CLICK-gelatin, independent of TSP-2 siRNA use, also appeared to decrease TSP-2 mRNA expression and protein expression, as well as decrease adventitial neovascularization, although this did not ultimately result in a significant reduction of IH at 21 days. These findings in the CLICK-gelatin only group were unexpected but are likely related to the interaction between the gel and the vasa vasorum, which are blood microvessels that penetrate the adventitia and the outer media, supplying them with nutrients and oxygen, and are known to play an important role in the vessel response to injury and development of atherosclerosis (71). The perivascular application of the CLICK-gelatin likely disrupts the function of the vasa vasorum by obstruction, potentially interfering with the delivery of cell signals, and thus leading to a reduction in TSP-2 expression and neovascularization seen in our study. Furthermore, an “outside-in” hypothesis of vascular remodeling where the adventitial fibroblasts play a key role in responding to inflammatory signals and modulating responses and adventitial cell migration into the neointima during the inflammatory period has been described (44, 72, 73). The CLICK-gelatin hydrogel, which is in direct contact with the adventitia is likely to be disrupting this process, leading to the downregulation of inflammatory signals following vascular injury. A similar response pattern has been previously demonstrated with the use of external stents in vein grafts (74, 75).

This study has limitations that should be addressed. First, the balloon angioplasty model is used to mimic the changes that lead to IH and restenosis of grafts following lower extremity bypass and may not perfectly reflect the changes that occur after surgical manipulation of diseased vessels. However, this model provides important proof-of-concept results that will be implemented in future studies using large animal models of lower extremity revascularization which are currently ongoing. Additionally, our study only evaluated IH development at 21 days. It has been shown that it may take up to 3 months for the maximum development of IH and differ based on animal size, therefore the impact of IH modulation by TSP-2 siRNA may differ at a longer time point and on the model used (76). However, we expect that early changes in the cell biology related to IH development targeted by TSP-2 siRNA would suppress the overall response leading to similar reduction in IH at longer time points. Perivascular delivery may also lead to non-specific delivery to surrounding tissues. In our experiment CLICK-gelatin containing siRNA was applied circumferentially around the vessel, which also puts it in contact with surrounding perivascular and subcutaneous

tissue, therefore some siRNA would have also been delivered to these tissues as opposed to the vessel, thus reducing the amount actually delivered to the intended target. Additional studies to optimize CLICK-gelatin siRNA delivery, including changes in the CLICK-gelatin to improve its adherence to vascular tissue and the addition of an impermeable backing to promote unidirectional delivery, are currently ongoing.

In summary, we demonstrated the promising ability of CLICK-gelatin perivascular delivery of TSP-2 siRNA to successfully suppress TSP-2 expression and effectively modulate MMP-9, limiting the development of IH in a rat carotid angioplasty model.

Supplementary Material

Refer to Web version on PubMed Central for supplementary material.

Acknowledgments:

This work has been supported by grants from *The National Heart, Lung, and Blood Institute* of the National Institutes of Health under award number R01HL021796, R01HL086741, 5T32HL007734, and 5T35HL110843.

Data Availability Statement:

The data that support the findings of this study are available in the methods, results and supplementary material of this article. Additional data are available from the corresponding authors upon reasonable request.

References

1. Chen G, Farris MS, Cowling T, Pinto L, Rogoza RM, MacKinnon E, Champsi S, and Anderson TJ (2021) Prevalence of atherosclerotic cardiovascular disease and subsequent major adverse cardiovascular events in Alberta, Canada: A real-world evidence study. Clin Cardiol 44, 1613–1620 [PubMed: 34585767]
2. Herrington W, Lacey B, Sherliker P, Armitage J, and Lewington S (2016) Epidemiology of Atherosclerosis and the Potential to Reduce the Global Burden of Atherothrombotic Disease. Circ Res 118, 535–546 [PubMed: 26892956]
3. Vasan RS, Enserro DM, Xanthakis V, Beiser AS, and Seshadri S (2022) Temporal Trends in the Remaining Lifetime Risk of Cardiovascular Disease Among Middle-Aged Adults Across 6 Decades: The Framingham Study. Circulation 145, 1324–1338 [PubMed: 35430874]
4. Nehler MR, Duval S, Diao L, Annex BH, Hiatt WR, Rogers K, Zakharyan A, and Hirsch AT (2014) Epidemiology of peripheral arterial disease and critical limb ischemia in an insured national population. J Vasc Surg 60, 686–695 e682 [PubMed: 24820900]
5. Mills JL Sr., Conte MS, Armstrong DG, Pomposelli FB, Schanzer A, Sidawy AN, Andros G, and Society for Vascular Surgery Lower Extremity Guidelines, C. (2014) The Society for Vascular Surgery Lower Extremity Threatened Limb Classification System: risk stratification based on wound, ischemia, and foot infection (WIfI). J Vasc Surg 59, 220–234 e221-222 [PubMed: 24126108]
6. Yusuf S, Zucker D, Peduzzi P, Fisher LD, Takaro T, Kennedy JW, Davis K, Killip T, Passamani E, Norris R, and et al. (1994) Effect of coronary artery bypass graft surgery on survival: overview of 10-year results from randomised trials by the Coronary Artery Bypass Graft Surgery Trialists Collaboration. Lancet 344, 563–570 [PubMed: 7914958]
7. Hachamovitch R, Hayes SW, Friedman JD, Cohen I, and Berman DS (2003) Comparison of the short-term survival benefit associated with revascularization compared with medical therapy in

patients with no prior coronary artery disease undergoing stress myocardial perfusion single photon emission computed tomography. Circulation 107, 2900–2907 [PubMed: 12771008]

8. Klinkert P, Schepers A, Burger DH, van Bockel JH, and Breslau PJ (2003) Vein versus polytetrafluoroethylene in above-knee femoropopliteal bypass grafting: five-year results of a randomized controlled trial. J Vasc Surg 37, 149–155 [PubMed: 12514593]
9. Pomposelli FB, Kansal N, Hamdan AD, Belfield A, Sheahan M, Campbell DR, Skillman JJ, and Logerfo FW (2003) A decade of experience with dorsalis pedis artery bypass: analysis of outcome in more than 1000 cases. J Vasc Surg 37, 307–315 [PubMed: 12563200]
10. Alexander JH, Hafley G, Harrington RA, Peterson ED, Ferguson TB Jr., Lorenz TJ, Goyal A, Gibson M, Mack MJ, Gennevois D, Califf RM, Kouchoukos NT, and Investigators, P. I. (2005) Efficacy and safety of edifoligide, an E2F transcription factor decoy, for prevention of vein graft failure following coronary artery bypass graft surgery: PREVENT IV: a randomized controlled trial. JAMA 294, 2446–2454 [PubMed: 16287955]
11. Conte MS, Bandyk DF, Clowes AW, Moneta GL, Seely L, Lorenz TJ, Namini H, Hamdan AD, Roddy SP, Belkin M, Berceli SA, DeMasi RJ, Samson RH, Berman SS, and Investigators, P. I. (2006) Results of PREVENT III: a multicenter, randomized trial of edifoligide for the prevention of vein graft failure in lower extremity bypass surgery. J Vasc Surg 43, 742–751; discussion 751 [PubMed: 16616230]
12. Owens CD, Gasper WJ, Rahman AS, and Conte MS (2015) Vein graft failure. J Vasc Surg 61, 203–216 [PubMed: 24095042]
13. Caliskan E, de Souza DR, Boning A, Liakopoulos OJ, Choi YH, Pepper J, Gibson CM, Perrault LP, Wolf RK, Kim KB, and Emmert MY (2020) Saphenous vein grafts in contemporary coronary artery bypass graft surgery. Nat Rev Cardiol 17, 155–169 [PubMed: 31455868]
14. Kapadia MR, Popowich DA, and Kibbe MR (2008) Modified prosthetic vascular conduits. Circulation 117, 1873–1882 [PubMed: 18391121]
15. Scharn DM, Daamen WF, van Kuppevelt TH, and van der Vliet JA (2012) Biological mechanisms influencing prosthetic bypass graft patency: possible targets for modern graft design. Eur J Vasc Endovasc Surg 43, 66–72 [PubMed: 22001149]
16. Cantelmo NL, Quist WC, and Lo Gerfo FW (1989) Quantitative analysis of anastomotic intimal hyperplasia in paired Dacron and PTFE grafts. J Cardiovasc Surg (Torino) 30, 910–915
17. Davies MG, and Hagen PO (1994) Pathobiology of intimal hyperplasia. Br J Surg 81, 1254–1269 [PubMed: 7953384]
18. Allaire E, and Clowes AW (1997) Endothelial cell injury in cardiovascular surgery: the intimal hyperplastic response. Ann Thorac Surg 63, 582–591 [PubMed: 9033355]
19. Bhardwaj S, Roy H, Heikura T, and Yla-Herttuala S (2005) VEGF-A, VEGF-D and VEGF-D(DeltaNDeltaC) induced intimal hyperplasia in carotid arteries. Eur J Clin Invest 35, 669–676 [PubMed: 16269016]
20. Bruczko M, Wolanska M, Malkowski A, Sobolewski K, and Kowalewski R (2016) Evaluation of Vascular Endothelial Growth Factor and Its Receptors in Human Neointima. Pathobiology 83, 47–52 [PubMed: 26890264]
21. Newby AC (2006) Matrix metalloproteinases regulate migration, proliferation, and death of vascular smooth muscle cells by degrading matrix and non-matrix substrates. Cardiovasc Res 69, 614–624 [PubMed: 16266693]
22. Hao H, Gabbiani G, and Bochaton-Piallat ML (2003) Arterial smooth muscle cell heterogeneity: implications for atherosclerosis and restenosis development. Arterioscler Thromb Vasc Biol 23, 1510–1520 [PubMed: 12907463]
23. de Vries MR, Simons KH, Jukema JW, Braun J, and Quax PH (2016) Vein graft failure: from pathophysiology to clinical outcomes. Nat Rev Cardiol 13, 451–470 [PubMed: 27194091]
24. Belkin N, Stoecker JB, Jackson BM, Damrauer SM, Glaser J, Kalapatapu V, Golden MA, and Wang GJ (2021) Effects of dual antiplatelet therapy on graft patency after lower extremity bypass. J Vasc Surg 73, 930–939 [PubMed: 32777321]
25. Bhasin M, Huang Z, Pradhan-Nabzdyk L, Malek JY, LoGerfo PJ, Contreras M, Guthrie P, Csizmadia E, Andersen N, Kocher O, Ferran C, and LoGerfo FW (2012) Temporal network

based analysis of cell specific vein graft transcriptome defines key pathways and hub genes in implantation injury. PLoS One 7, e39123 [PubMed: 22720046]

26. Willis DJ, Kalish JA, Li C, Deutsch ER, Contreras MA, LoGerfo FW, and Quist WC (2004) Temporal gene expression following prosthetic arterial grafting. J Surg Res 120, 27–36 [PubMed: 15172187]
27. Yoshida S, Nabzdyk CS, Pradhan L, and LoGerfo FW (2011) Thrombospondin-2 gene silencing in human aortic smooth muscle cells improves cell attachment. J Am Coll Surg 213, 668–676 [PubMed: 21840228]
28. Bodewes TC, Johnson JM, Auster M, Huynh C, Muralidharan S, Contreras M, LoGerfo FW, and Pradhan-Nabzdyk L (2017) Intraluminal delivery of thrombospondin-2 small interfering RNA inhibits the vascular response to injury in a rat carotid balloon angioplasty model. FASEB J 31, 109–119 [PubMed: 27671229]
29. Malik N, Francis SE, Holt CM, Gunn J, Thomas GL, Shepherd L, Chamberlain J, Newman CM, Cumberland DC, and Crossman DC (1998) Apoptosis and cell proliferation after porcine coronary angioplasty. Circulation 98, 1657–1665 [PubMed: 9778332]
30. Tasaki T, Yamada S, Guo X, Tanimoto A, Wang KY, Nabeshima A, Kitada S, Noguchi H, Kimura S, Shimajiri S, Kohno K, Ichijo H, and Sasaguri Y (2013) Apoptosis signal-regulating kinase 1 deficiency attenuates vascular injury-induced neointimal hyperplasia by suppressing apoptosis in smooth muscle cells. Am J Pathol 182, 597–609 [PubMed: 23178077]
31. Cho A, and Reidy MA (2002) Matrix metalloproteinase-9 is necessary for the regulation of smooth muscle cell replication and migration after arterial injury. Circ Res 91, 845–851 [PubMed: 12411400]
32. Watanabe R, Maeda T, Zhang H, Berry GJ, Zeisbrich M, Brockett R, Greenstein AE, Tian L, Goronzy JJ, and Weyand CM (2018) MMP (Matrix Metalloprotease)-9-Producing Monocytes Enable T Cells to Invade the Vessel Wall and Cause Vasculitis. Circ Res 123, 700–715 [PubMed: 29970365]
33. Kwei S, Stavrakis G, Takahas M, Taylor G, Folkman MJ, Gimbrone MA Jr., and Garcia-Cardena G (2004) Early adaptive responses of the vascular wall during venous arterialization in mice. Am J Pathol 164, 81–89 [PubMed: 14695322]
34. Weaver H, Shukla N, Ellinsworth D, and Jeremy JY (2012) Oxidative stress and vein graft failure: a focus on NADH oxidase, nitric oxide and eicosanoids. Curr Opin Pharmacol 12, 160–165 [PubMed: 22503078]
35. Osgood MJ, Hocking KM, Voskresensky IV, Li FD, Komalavilas P, Cheung-Flynn J, and Brophy CM (2014) Surgical vein graft preparation promotes cellular dysfunction, oxidative stress, and intimal hyperplasia in human saphenous vein. J Vasc Surg 60, 202–211 [PubMed: 23911244]
36. Bornstein P, Agah A, and Kyriakides TR (2004) The role of thrombospondins 1 and 2 in the regulation of cell-matrix interactions, collagen fibril formation, and the response to injury. Int J Biochem Cell Biol 36, 1115–1125 [PubMed: 15094126]
37. Deglise S, Bechelli C, and Allagnat F (2022) Vascular smooth muscle cells in intimal hyperplasia, an update. Front Physiol 13, 1081881 [PubMed: 36685215]
38. Helkin A, Maier KG, and Gahtan V (2015) Thrombospondin-1, −2 and −5 have differential effects on vascular smooth muscle cell physiology. Biochem Biophys Res Commun 464, 1022–1027 [PubMed: 26168731]
39. Liu JF, Chen PC, Chang TM, and Hou CH (2020) Thrombospondin-2 stimulates MMP-9 production and promotes osteosarcoma metastasis via the PLC, PKC, c-Src and NF-kappaB activation. J Cell Mol Med 24, 12826–12839 [PubMed: 33021341]
40. Cheng L, Mantile G, Pauly R, Nater C, Felici A, Monticone R, Bilato C, Gluzband YA, Crow MT, Stetler-Stevenson W, and Capogrossi MC (1998) Adenovirus-mediated gene transfer of the human tissue inhibitor of metalloproteinase-2 blocks vascular smooth muscle cell invasiveness in vitro and modulates neointimal development in vivo. Circulation 98, 2195–2201 [PubMed: 9815875]
41. Tellechea A, Leal EC, Kafanas A, Auster ME, Kuchibhotla S, Ostrovsky Y, Tecilazich F, Baltzis D, Zheng Y, Carvalho E, Zabolotny JM, Weng Z, Petra A, Patel A, Panagiotidou S, Pradhan-Nabzdyk L, Theoharides TC, and Veves A (2016) Mast Cells Regulate Wound Healing in Diabetes. Diabetes 65, 2006–2019 [PubMed: 27207516]

42. Westerband A, Gentile AT, Hunter GC, Gooden MA, Aguirre ML, Berman SS, and Mills JL (2000) Intimal growth and neovascularization in human stenotic vein grafts. J Am Coll Surg 191, 264–271 [PubMed: 10989901]
43. Bogdanov L, Shishkova D, Mukhamadiyarov R, Velikanova E, Tsepokina A, Terekhov A, Koshelev V, Kanonykina A, Shabaev A, Frolov A, Zagorodnikov N, and Kutikhin A (2022) Excessive Adventitial and Perivascular Vascularisation Correlates with Vascular Inflammation and Intimal Hyperplasia. Int J Mol Sci 23
44. Damrauer SM, Fisher MD, Wada H, Siracuse JJ, da Silva CG, Moon K, Csizmadia E, Maccariello ER, Patel VI, Studer P, Essayagh S, Aird WC, Daniel S, and Ferran C (2010) A20 inhibits post-angioplasty restenosis by blocking macrophage trafficking and decreasing adventitial neovascularization. Atherosclerosis 211, 404–408 [PubMed: 20430393]
45. Fleiner M, Kummer M, Mirlacher M, Sauter G, Cathomas G, Krapf R, and Biedermann BC (2004) Arterial neovascularization and inflammation in vulnerable patients: early and late signs of symptomatic atherosclerosis. Circulation 110, 2843–2850 [PubMed: 15505090]
46. Moulton KS, Vakili K, Zurakowski D, Soliman M, Butterfield C, Sylvin E, Lo KM, Gillies S, Javaherian K, and Folkman J (2003) Inhibition of plaque neovascularization reduces macrophage accumulation and progression of advanced atherosclerosis. Proc Natl Acad Sci U S A 100, 4736–4741 [PubMed: 12682294]
47. Gu C, Lhamo T, Zou C, Zhou C, Su T, Draga D, Luo D, Zheng Z, Yin L, and Qiu Q (2020) Comprehensive analysis of angiogenesis-related genes and pathways in early diabetic retinopathy. BMC Med Genomics 13, 142 [PubMed: 32993645]
48. Zhang Y, Cao J, Zhou J, Zhang C, Li Q, Chen S, Feinstein S, Grayburn PA, and Huang P (2021) Plaque Elasticity and Intraplaque Neovascularisation on Carotid Artery Ultrasound: A Comparative Histological Study. Eur J Vasc Endovasc Surg 62, 358–366 [PubMed: 34266763]
49. Drinane M, Mollmark J, Zagorchev L, Moodie K, Sun B, Hall A, Shipman S, Morganelli P, Simons M, and Mulligan-Kehoe MJ (2009) The antiangiogenic activity of rPAI-1(23) inhibits vasa vasorum and growth of atherosclerotic plaque. Circ Res 104, 337–345 [PubMed: 19122176]
50. Mollmark J, Ravi S, Sun B, Shipman S, Buitendijk M, Simons M, and Mulligan-Kehoe MJ (2011) Antiangiogenic activity of rPAI-1(23) promotes vasa vasorum regression in hypercholesterolemic mice through a plasmin-dependent mechanism. Circ Res 108, 1419–1428 [PubMed: 21546607]
51. Herrmann J, Lerman LO, Rodriguez-Porcel M, Holmes DR Jr., Richardson DM, Ritman EL, and Lerman A (2001) Coronary vasa vasorum neovascularization precedes epicardial endothelial dysfunction in experimental hypercholesterolemia. Cardiovasc Res 51, 762–766 [PubMed: 11530109]
52. Lavin B, Gomez M, Pello OM, Castejon B, Piedras MJ, Saura M, and Zaragoza C (2014) Nitric oxide prevents aortic neointimal hyperplasia by controlling macrophage polarization. Arterioscler Thromb Vasc Biol 34, 1739–1746 [PubMed: 24925976]
53. Zhang Y, Fu Y, Zhang C, Jia L, Yao N, Lin Y, Dong Y, Fatima N, Alam N, Wang R, Wang W, Bai L, Zhao S, and Liu E (2021) MED1 Deficiency in Macrophages Accelerates Intimal Hyperplasia via ROS Generation and Inflammation. Oxid Med Cell Longev 2021, 3010577 [PubMed: 34853629]
54. Korshunov VA, Nikonenko TA, Tkachuk VA, Brooks A, and Berk BC (2006) Interleukin-18 and macrophage migration inhibitory factor are associated with increased carotid intima-media thickening. Arterioscler Thromb Vasc Biol 26, 295–300 [PubMed: 16293799]
55. Murphy-Ullrich JE, and Suto MJ (2018) Thrombospondin-1 regulation of latent TGF-beta activation: A therapeutic target for fibrotic disease. Matrix Biol 68-69, 28–43 [PubMed: 29288716]
56. Kim JS, Kim JG, Moon MY, Jeon CY, Won HY, Kim HJ, Jeon YJ, Seo JY, Kim JI, Kim J, Lee JY, Kim PH, and Park JB (2006) Transforming growth factor-beta1 regulates macrophage migration via RhoA. Blood 108, 1821–1829 [PubMed: 16705092]
57. Li MO, Wan YY, Sanjabi S, Robertson AK, and Flavell RA (2006) Transforming growth factor-beta regulation of immune responses. Annu Rev Immunol 24, 99–146 [PubMed: 16551245]
58. Letterio JJ, and Roberts AB (1998) Regulation of immune responses by TGF-beta. Annu Rev Immunol 16, 137–161 [PubMed: 9597127]

59. Guo N, Krutzsch HC, Inman JK, and Roberts DD (1997) Thrombospondin 1 and type I repeat peptides of thrombospondin 1 specifically induce apoptosis of endothelial cells. Cancer Res 57, 1735–1742 [PubMed: 9135017]
60. Jimenez B, Volpert OV, Crawford SE, Febbraio M, Silverstein RL, and Bouck N (2000) Signals leading to apoptosis-dependent inhibition of neovascularization by thrombospondin-1. Nat Med 6, 41–48 [PubMed: 10613822]
61. Chu XD, Lin ZB, Huang T, Ding H, Zhang YR, Zhao Z, Huangfu SC, Qiu SH, Guo YG, Chu XL, Pan JH, and Pan YL (2022) Thrombospondin-2 holds prognostic value and is associated with metastasis and the mismatch repair process in gastric cancer. BMC Cancer 22, 250 [PubMed: 35255858]
62. Streit M, Riccardi L, Velasco P, Brown LF, Hawighorst T, Bornstein P, and Detmar M (1999) Thrombospondin-2: a potent endogenous inhibitor of tumor growth and angiogenesis. Proc Natl Acad Sci U S A 96, 14888–14893 [PubMed: 10611308]
63. Koch M, Hussein F, Woeste A, Grundker C, Frontzek K, Emons G, and Hawighorst T (2011) CD36-mediated activation of endothelial cell apoptosis by an N-terminal recombinant fragment of thrombospondin-2 inhibits breast cancer growth and metastasis in vivo. Breast Cancer Res Treat 128, 337–346 [PubMed: 20714802]
64. Bartoli F, Debant M, Chuntharpursat-Bon E, Evans EL, Musialowski KE, Parsonage G, Morley LC, Futers TS, Sukumar P, Bowen TS, Kearney MT, Lichtenstein L, Roberts LD, and Beech DJ (2022) Endothelial Piezo1 sustains muscle capillary density and contributes to physical activity. J Clin Invest 132
65. Walsh K, Smith RC, and Kim HS (2000) Vascular cell apoptosis in remodeling, restenosis, and plaque rupture. Circ Res 87, 184–188 [PubMed: 10926867]
66. Wang CH, Verma S, Hsieh IC, Hung A, Cheng TT, Wang SY, Liu YC, Stanford WL, Weisel RD, Li RK, and Cherng WJ (2007) Stem cell factor attenuates vascular smooth muscle apoptosis and increases intimal hyperplasia after vascular injury. Arterioscler Thromb Vasc Biol 27, 540–547 [PubMed: 17204664]
67. Koshy ST, Desai RM, Joly P, Li J, Bagrodia RK, Lewin SA, Joshi NS, and Mooney DJ (2016) Click-Crosslinked Injectable Gelatin Hydrogels. Adv Healthc Mater 5, 541–547 [PubMed: 26806652]
68. Khunawattanakul W, Jaipakdee N, Rongthong T, Chansri N, Srisuk P, Chitropas P, and Pongjanyakul T (2022) Sodium Alginate-Quaternary Polymethacrylate Composites: Characterization of Dispersions and Calcium Ion Cross-Linked Gel Beads. Gels 8
69. Yang S, Tutton S, Pierce E, and Yoon K (2001) Specific double-stranded RNA interference in undifferentiated mouse embryonic stem cells. Mol Cell Biol 21, 7807–7816 [PubMed: 11604515]
70. Mocellin S, and Provenzano M (2004) RNA interference: learning gene knock-down from cell physiology. J Transl Med 2, 39 [PubMed: 15555080]
71. Boyle EC, Sedding DG, and Haverich A (2017) Targeting vasa vasorum dysfunction to prevent atherosclerosis. Vascul Pharmacol 96-98, 5–10 [PubMed: 28830735]
72. Maiellaro K, and Taylor WR (2007) The role of the adventitia in vascular inflammation. Cardiovasc Res 75, 640–648 [PubMed: 17662969]
73. Scott NA, Cipolla GD, Ross CE, Dunn B, Martin FH, Simonet L, and Wilcox JN (1996) Identification of a potential role for the adventitia in vascular lesion formation after balloon overstretch injury of porcine coronary arteries. Circulation 93, 2178–2187 [PubMed: 8925587]
74. Yasuda S, Goda M, Shibuya T, Uchida K, Suzuki S, Noishiki Y, Yokoyama U, Ishikawa Y, and Masuda M (2019) An appropriately sized soft polyester external stent prevents enlargement and neointimal hyperplasia of a saphenous vein graft in a canine model. Artif Organs 43, 577–583 [PubMed: 30488514]
75. Yang Q, Lei D, Huang S, Yang Y, Yang Y, Ye X, You Z, and Zhao Q (2020) Effects of the different-sized external stents on vein graft intimal hyperplasia and inflammation. Ann Transl Med 8, 102 [PubMed: 32175395]
76. Lemson MS, Tordoir JH, Daemen MJ, and Kitslaar PJ (2000) Intimal hyperplasia in vascular grafts. Eur J Vasc Endovasc Surg 19, 336–350 [PubMed: 10801366]

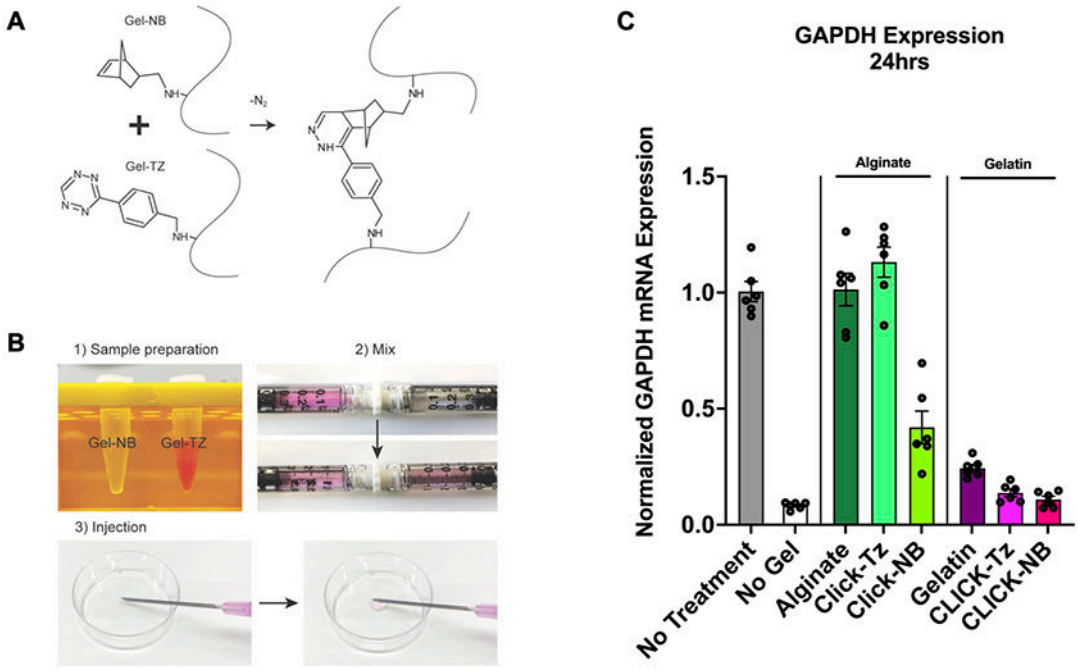

Figure 1.

CLICK-Gelatin synthesis and physical characterization and siRNA transfection efficacy in vitro. a) Gelatin polymers were modified with norbornene (NB) and tetrazine (Tz) groups and spontaneously formed stable crosslinked CLICK-Gelatin when combined. b) Gel-NB and Gel-Tz polymers can be dissolved rapidly at room temperature in PBS, mixed, and applied to intended target prior to hydrogel formation. C) Relative gene expression of GAPDH following GAPDH siRNA transfection at 48 hrs. Fold change in GAPDH mRNA expression normalized to nontreated (NT) ECs at 48hrs and compare to positive control (no gel), and all experimental groups. Data are presented as means +/− SEM; n = 6. *P ≤ 0.05.

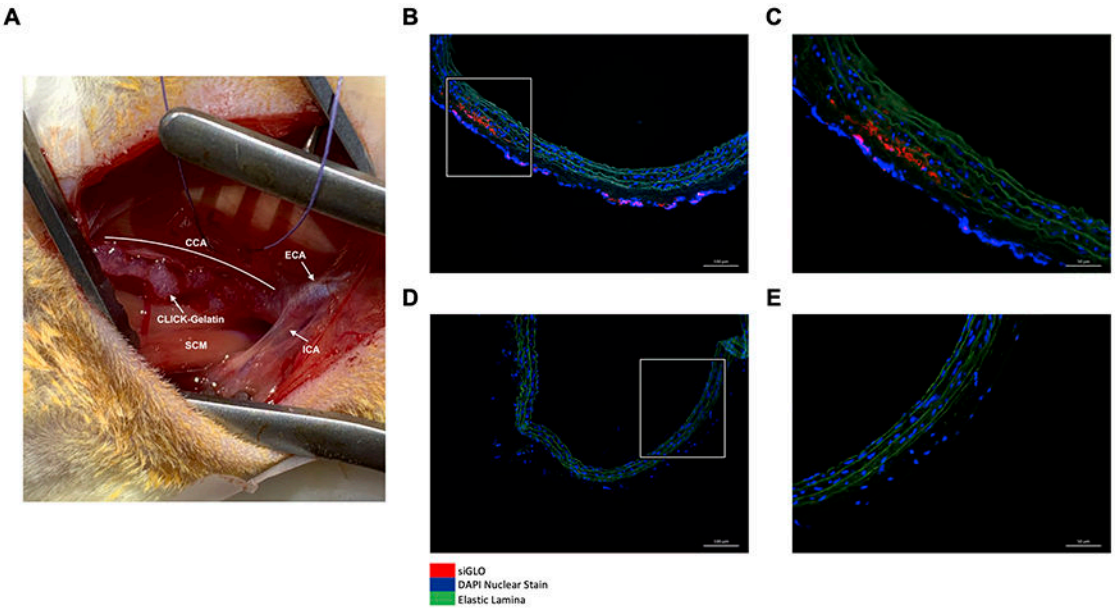

Figure 2.

siGLO delivery and expression at 48hrs after CLICK-Gelatin mediated perivascular delivery. A) Delivery of siGLO embedded CLICK-Gelatin to rat CCA following denudation. B,C) Representative images of effective siGLO delivery to a rat CCA tunica adventitia and media 48hrs following denudation and perivascular delivery of CLICK-Gel embedded with siGLO. D,E) Contralateral CCA represented as negative control. Images were stained for siGLO (red epifluorescence), nuclei (blue), and elastic lamina (green autofluorescence). White boxes represent area of magnification. Original magnification, x200 (A,C), x400 (B,D). Scale bars, 100 μm (A,C) and 50μm (B,D).

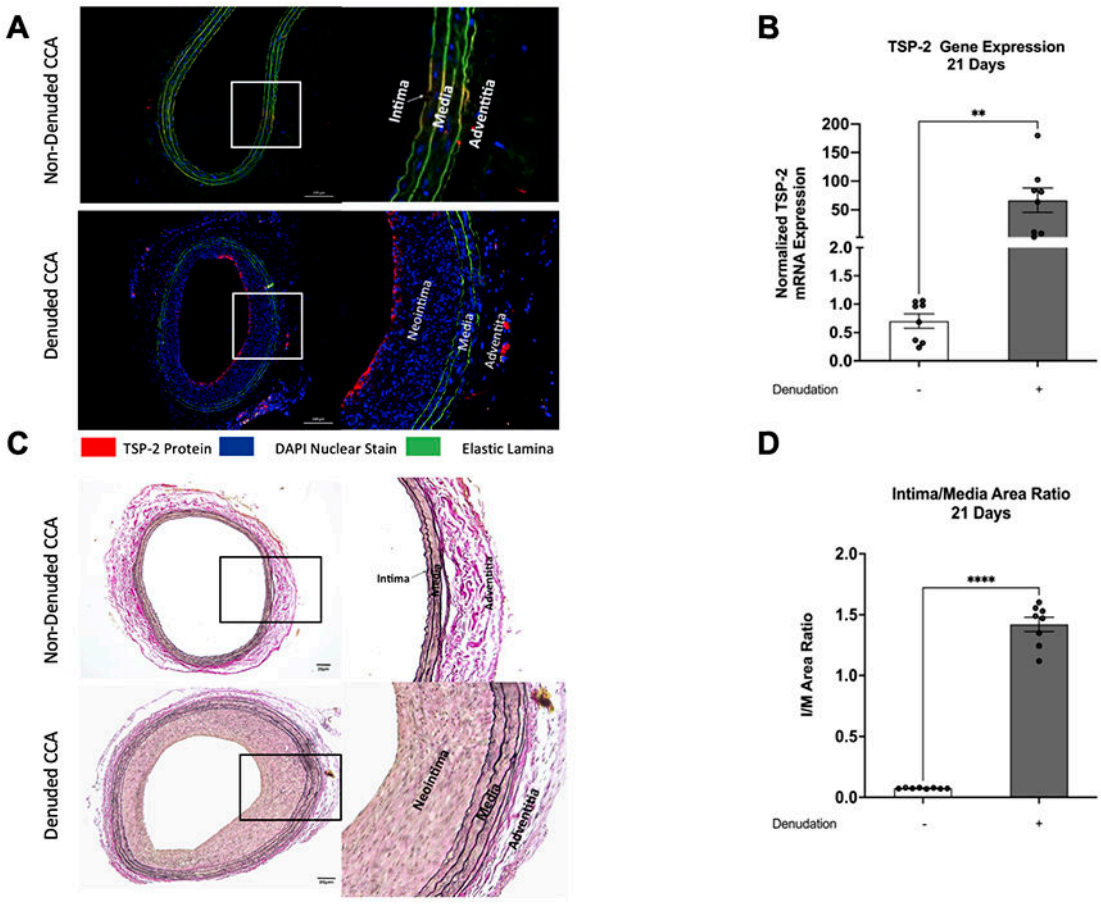

Figure 3.

Effects of Denudation in Rat Carotid Artery. A) TSP-2 protein and B) mRNA expression and C,D) development of IH at 21d following balloon denudation of CCA. Data are presented as means +/−SEM; n = 8. *P ≤ 0.05.

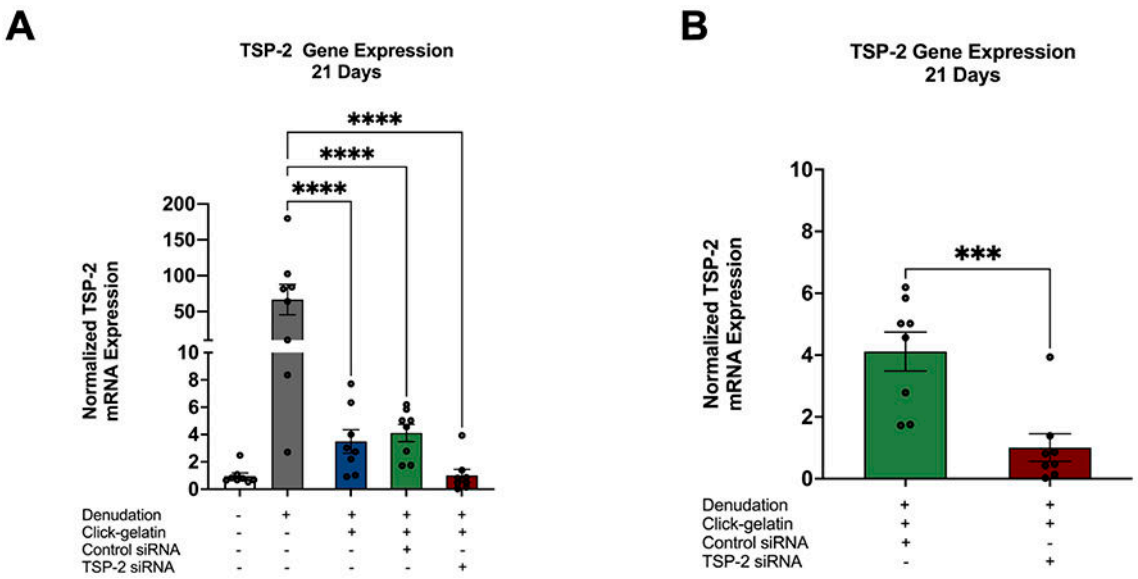

Figure 4.

Relative gene expression of TSP-2. Fold change in TSP-2 mRNA expression normalized to nondenuded contralateral CCA at 21 d and compared across all groups (A), and treatment only groups and negative control group B). Data are presented as means +/−SEM; n = 8. *P ≤ 0.05.

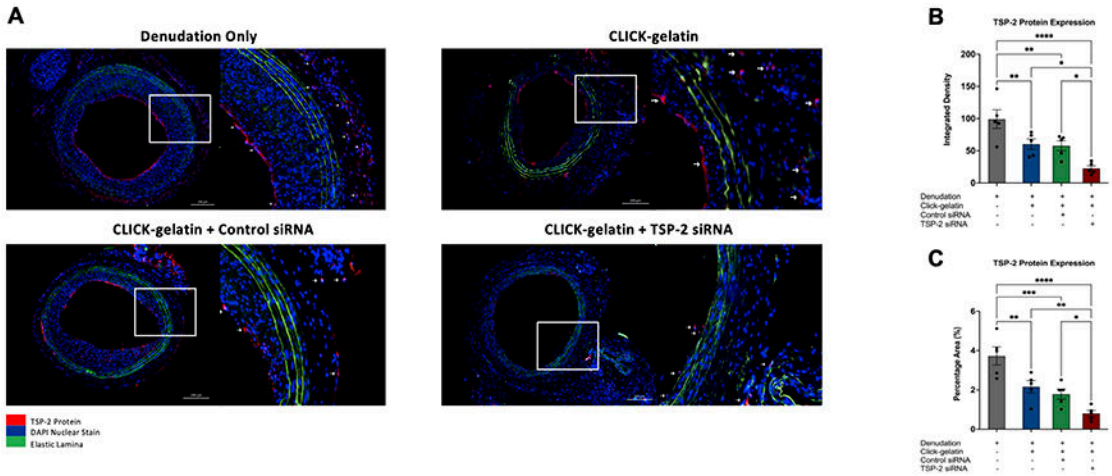

Figure 5.

TSP-2 protein expression. A) Representative images at 21 d of all denuded CCA stained for TSP-2 protein (red), nuclei (blue), and elastic lamina (green autofluorescence). B,C) Quantification of TSP-2 protein expression in all groups at 21 d on the basis of density (B) and dissemination area (C). Data are presented as means +/−SEM; n = 4. Original magnification, x100. Scale bars, 200 μm. *P≤ 0.05.

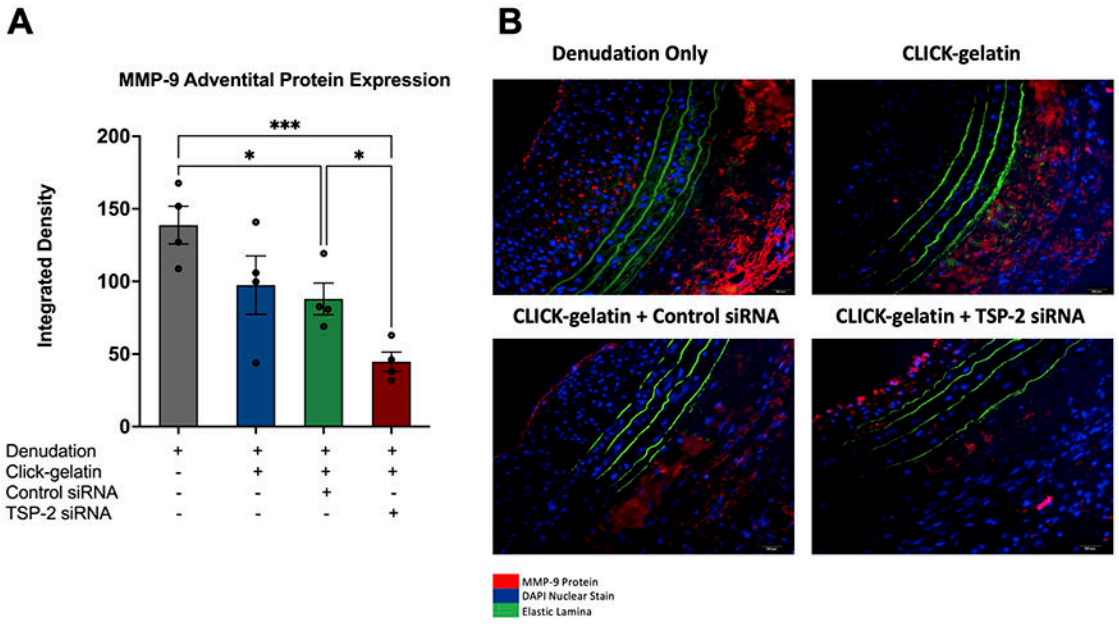

Figure 6.

MMP-9 protein expression. Quantification of MMP-9 protein expression in all groups at 21 d on the basis of integrated density (signal strength), (A). Data are presented as means +/− SEM; n = 4. B) Representative images at 21 d of all denuded CCA stained for MMP-9 protein (red), nuclei (blue), and elastic lamina (green autofluorescence). Original magnification, x400. Scale bars, 20 μm. *P≤0.05.

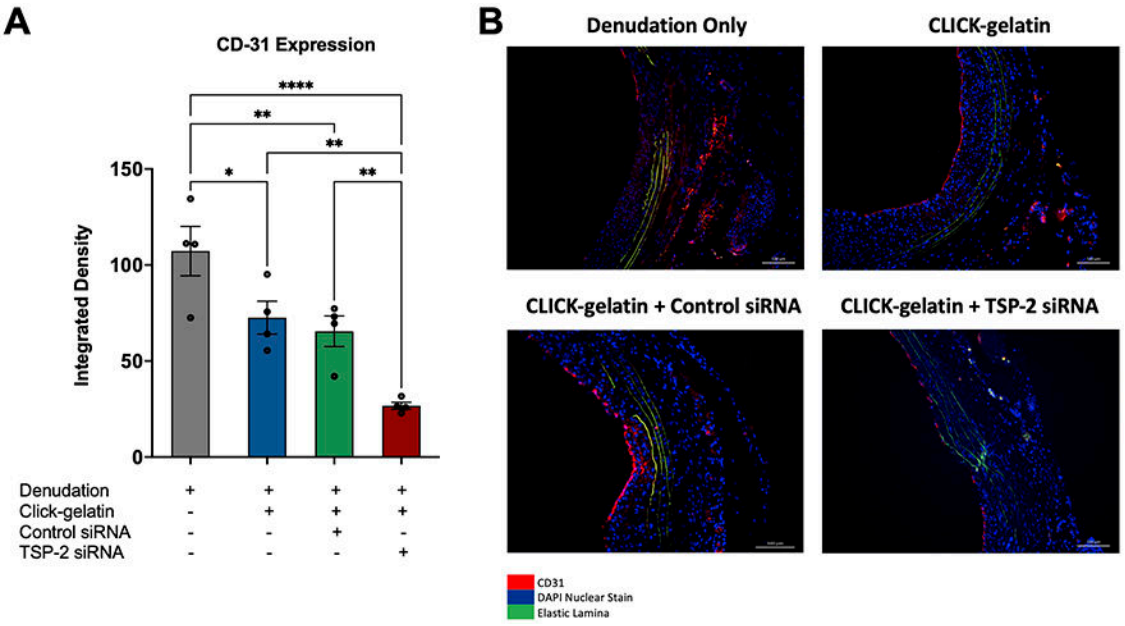

Figure 7.

CD31 protein expression. Quantification of CD31 protein expression in all groups at 21 d on the basis of density scores (A). Data are presented as means +/− SEM; n = 4. B) Representative images at 21 d of all denuded CCA stained for CD31 protein (red), nuclei (blue), and elastic lamina (green autofluorescence). Original magnification, x200. Scale bars, 100 μm. *P≤0.05.

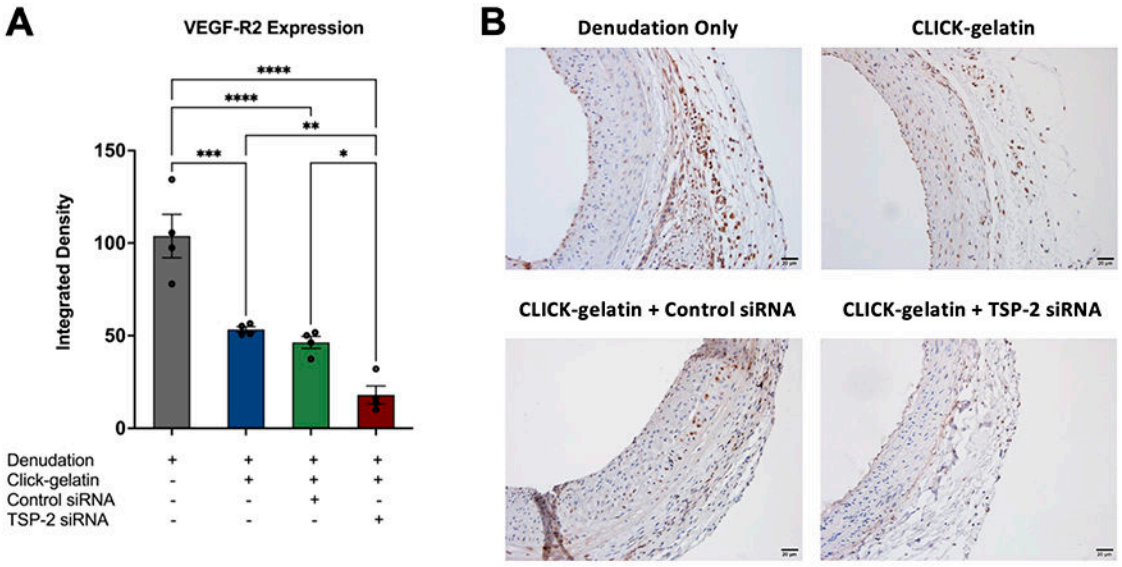

Figure 8.

VEGF-R2 expression. Quantification of VEGF-R2 expression in all groups at 21 d on the basis of density scores (A). Data are presented as means +/− SEM; n = 4. C) Representative images at 21 d of all denuded CCA stained for VEGF-R2 (brown), nuclei (blue). Original magnification, x200. Scale bars, 20 μm. *P≤ 0.05.

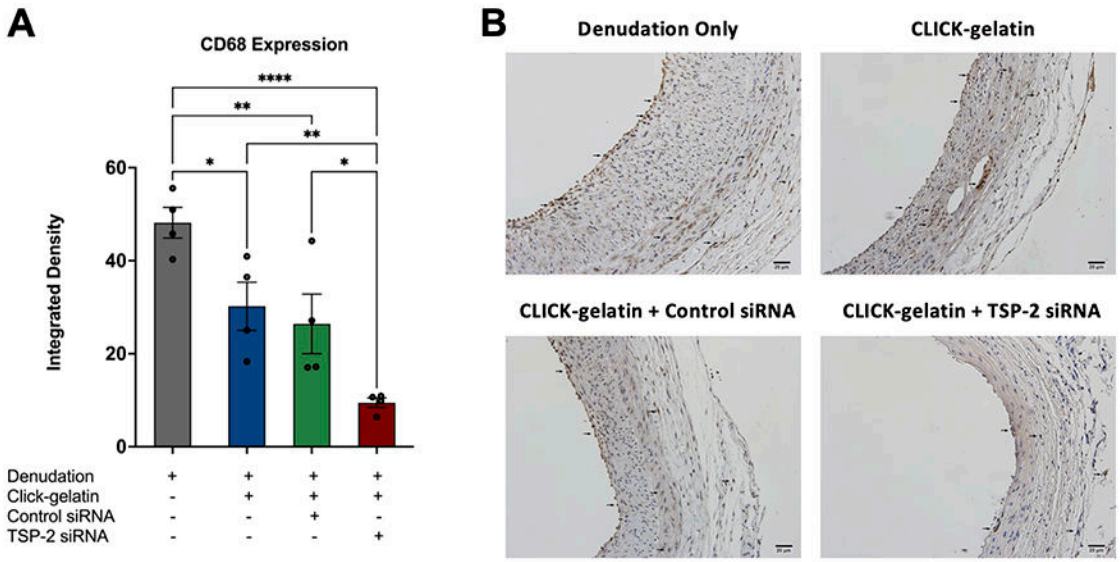

Figure 9.

CD68 expression. Quantification of CD68 expression in all groups at 21 d on the basis of density scores (A). Data are presented as means +/− SEM; n = 4. C) Representative images at 21 d of all denuded CCA stained for CD68 (brown), nuclei (blue). Original magnification, x200. Scale bars, 20 μm. *P ≤ 0.05.

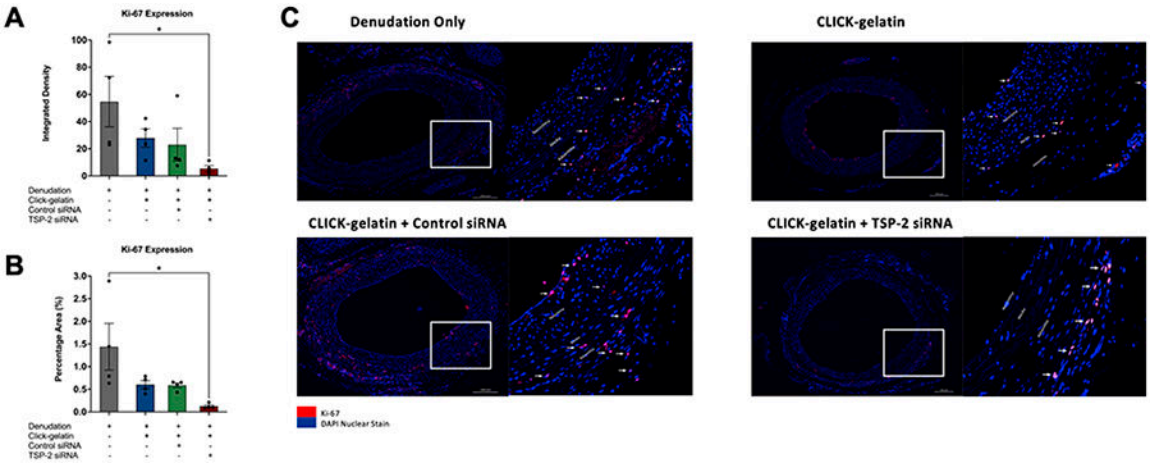

Figure 10.

Ki-67 protein expression. Quantification of Ki-67 protein expression in all groups at 21 d on the basis of density scores (A). Data are presented as means +/− SEM; n = 4; Ki-67 protein expression in all groups at 21 d on the basis of density (A) and dissemination area (B). . C) Representative images at 21 d of all denuded CCA stained for Ki-67 protein (red), nuclei (blue). Original magnification, x100. Scale bars, 200 μm. *P ≤ 0.05.

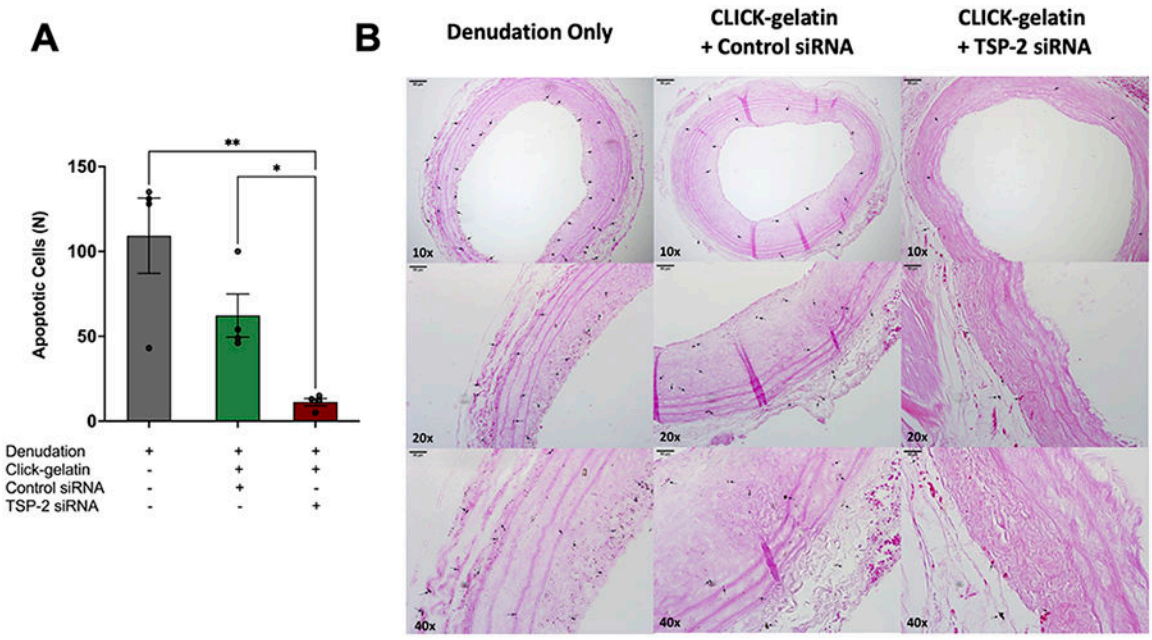

Figure 11.

Effect of Click-gelatin with TSP-2 siRNA on apoptosis. Quantification of apoptosis as determined by Terminal deoxynucleotidyl transferase dUTP nick end labelling (TUNEL) staining at 21 d. (A) Data are presented as means +/− SEM; n = 4. C) Representative images at 21 d of denuded CCA stained for DNA fragmentation (black). Scale bars, 50 μm. *P ≤ 0.05.

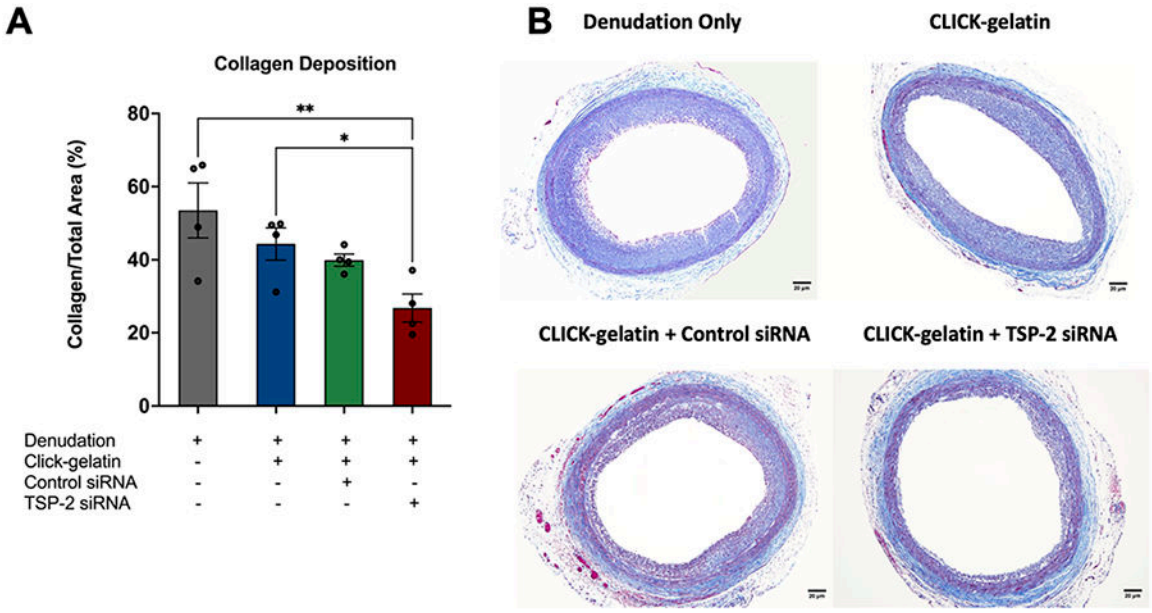

Figure 12.

Collagen deposition. A) Quantitative analysis of collagen deposition in all groups at 21 d expressed as a percentage of total area of the cross-section. Data are presented as means +/− SEM; n = 4. B) Representative images at 21 d of Masson's Trichrome–stained denuded CCA in all groups. Collagen (blue); cytoplasm, keratin, and muscle (red); and nuclei (black). Original magnification, x100. Scale bars, 20 mm. *P ≤0.05.

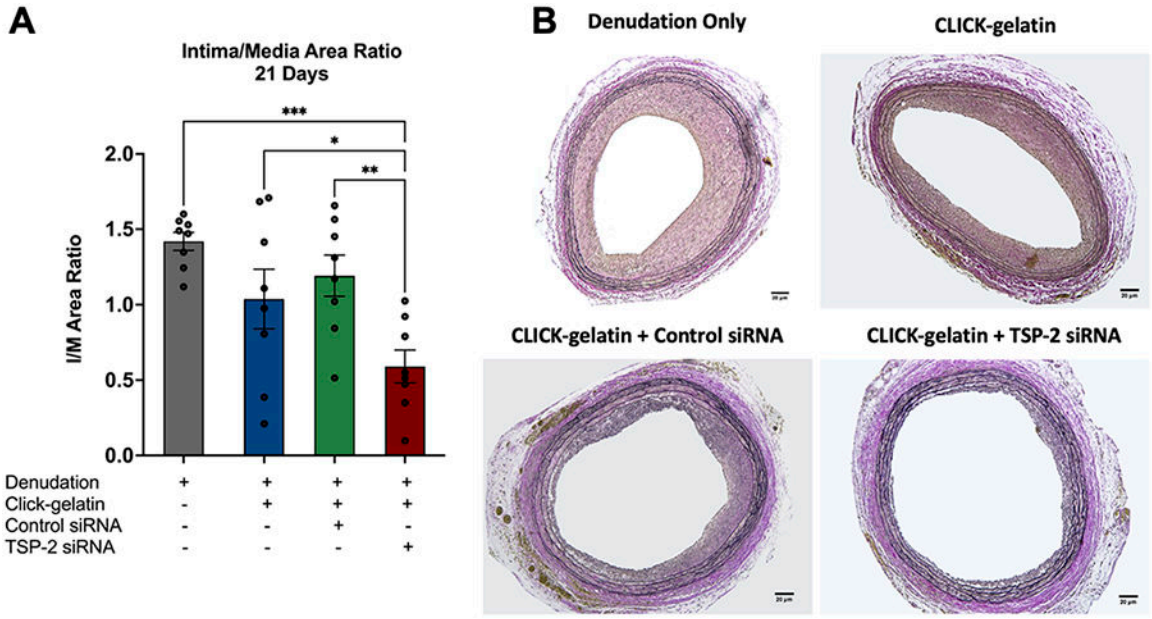

Figure 13.

Morphometric analysis of A) Intima/media area ratios in all groups at 21 d. Data are presented as means +/− SEM; n = 8. B) Representative cross-sections at 21 d of all groups. Sections were stained with Verhoef-van Giesson. Intima was defined by the area between lumen and inner elastic lamina, whereas the area between the inner and outer elastic lamina represents the media. Original magnification, x40. Scale bars, 20 μm. *P≤0.05.